THE JOURNAL OF PHYSICAL CHEMISTRY B

Article

pubs.acs.org/JPCB

A Universal Model of Restricted Diffusion for Fluorescence Correlation Spectroscopy

Tomasz K. Piskorz[†] and Anna Ochab-Marcinek*[,‡]

[†]Department of Chemistry, University of Warsaw, ul. Pasteura 1, 02-093 Warsaw, Poland

[‡]Institute of Physical Chemistry, Polish Academy of Sciences, ul. Kasprzaka 44/52, 01-224 Warsaw, Poland

Supporting Information

ABSTRACT: Fluorescence correlation spectroscopy (FCS) is frequently used to study the processes of restricted diffusion. The most important quantity to determine is the size of the structures that hinder the Brownian motion of the molecules. We study three qualitatively different models of restricted diffusion, widely applied in biophysics and material science: Diffusion constrained by elastic force (i), walking confined diffusion (ii), and hop diffusion (iii). They cover the diversity of statistical behaviors, from purely Gaussian (i) to sharply non-Gaussian on intermediate time scales (ii) and, additionally, discrete (iii). We test whether one can use the Gaussian approximation of the FCS autocorrelation function to interpret the non-Gaussian data. We show that (i−iii) have approximately the same mean square displacements. Using simulations, we show that the FCS data suspected of restricted diffusion can be reliably interpreted using one archetypal model (i). Even if the underlying mechanism of the restriction is different or unknown, the accuracy of fitting the confinement size is excellent, and diffusion coefficients are also estimated with a good accuracy. This study gives a physical insight into the statistical behavior of different types of restricted diffusion and into the ability of fluorescence correlation spectroscopy to distinguish between them.

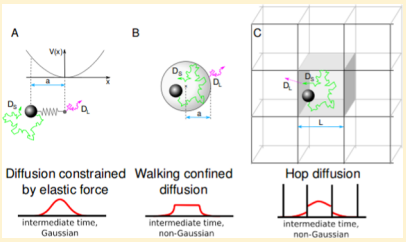

INTRODUCTION

Diffusion in crowded environments has recently been widely investigated in the fields of biophysics and polymer physics. The constraints imposed by the structure of the crowded medium reduce the diffusivity of molecules in a nontrivial way: The mean square displacement (or, equivalently, an effective time-dependent diffusion coefficient) depends nonlinearly on time. Fluorescence correlation spectroscopy (FCS) is a frequently used experimental technique for measuring the diffusion dynamics of particles in crowded media. In order to interpret the measurements, various theoretical models of restricted diffusion are assumed. For the systems where a transition is observed between two regimes of free diffusion (fast on a short time scale and slow at long times), three models are especially popular (Figure 1):

(i) Diffusion constrained by elastic force. The model describes an overdamped motion of a Brownian particle in a harmonic potential whose center freely diffuses through space. It is used in polymer physics, in the Rouse model of polymer dynamics[1] (monomers as beads on springs). Another example is diffusion of molecules in viscoelastic media,[2] e.g. in a solution of small polymers interacting with each other with noncovalent hydrogen bonds.[3] An effectively similar model was used to describe diffusion of particles in Jeffreys liquid.[4] Due to its simplicity, harmonic potential is also often arbitrarily assumed as the constraint for diffusion in living cells, e.g. to describe the mobility of DNA segments within the *Escherichia coli* nucleoid,[5] or the movement of opioid receptors on the plasma membrane in NRK cells.[6]

(ii) Walking confined diffusion. In this model, the Brownian particle moves inside a reflecting spherical (or circular) shell whose center freely diffuses. In polymer physics, this model has been used to describe the motion of nanoparticles in polymer solutions in the presence of a less crowded depletion layer around the particle.[7,8] In biophysics, the model has been used in the FCS measurements of synaptic vesicle movement within hypothetical cages.[9,10] A version of the model, where the circular (or cylindrical) confinement was immobile was used in the FCS study of diffusion of molecules inside dendrites.[11,12] There are also related studies where the model is not used explicitly, but the type of diffusion that can actually be detected in the experiment is the diffusion in a reflecting spherical shell: FCS measurements of diffusion of nanoparticles confined within aqueous droplets in microfluidic devices,[13] and of fluorescent molecules enclosed in nanocontainers;[14] single-particle tracking measurements of protein mobility in the cell nucleus[15] and of the mobility of polymersomes enclosed in larger polymersomes.[16]

(iii) Hop diffusion. The Brownian particle moves in a system of periodic permeable barriers. In a two-dimensional variant, this model has been widely used to describe the diffusion of proteins anchored in a cell membrane, where the membrane-associated cytoskeleton plays the role of

Received: March 11, 2014
Revised: April 17, 2014
Published: April 17, 2014

   dx.doi.org/10.1021/jp502467u | J. Phys. Chem. B 2014, 118, 4906−4912

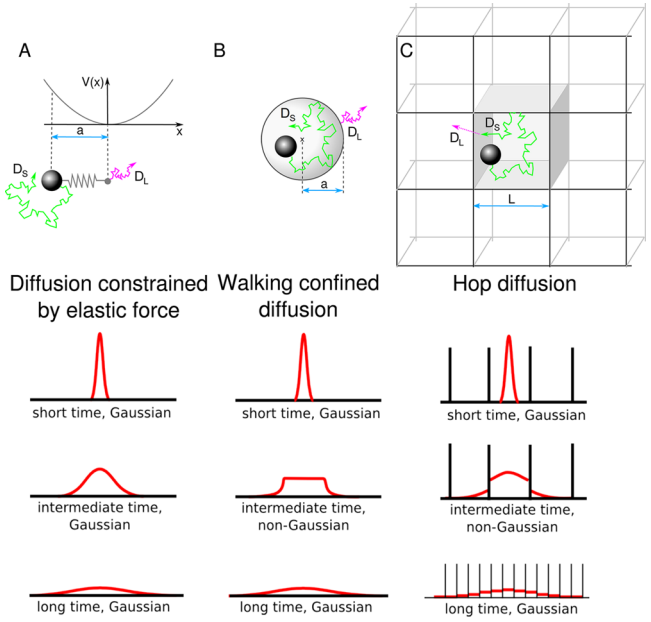

Figure 1. Models of confined diffusion. (A) Diffusion constrained by elastic force. The propagator of this process is Gaussian in all time scales. (B) Walking confined diffusion. (C) Hop diffusion. The propagators of the processes B and C are Gaussian only in the short- and long-time limits.

permeable fences.[17,18] The model has also been used in the simulation studies that analyzed the dependence of the diffusion half-time of the FCS autocorrelation curve on the size of the focal volume.[19] Approximations of FCS autocorrelation functions (ACF) in hop diffusion in various time scales have been studied by Destainville.[20] To our knowledge, the model of permeable membranes has not been used to date for description of three-dimensional diffusion inside living cells, but it might be useful to study diffusion in mitochondria or endoplasmatic reticulum as these structures are three-dimensional compartments divided by membranes. The model of permeable barriers can also be used as an approximation for diffusion in porous materials.[21] FCS measurements of diffusion in porous nanostructures have been done on inverse colloidal crystals,[22] and simulations of FCS experiments have been done on protein diffusion in lipid cubic phases.[23] Similar to (ii) or (iii) is the caging effect in polymer glasses[24] and melts,[25] where the molecule "rattles around" in an enclosure built by other molecules, and reflections from the cage walls temporarily increase the non-Gaussianity parameter of its position distribution. However, the picture of "rattling" was recently proved insufficient or even wrong in the case of lipid bilayers.[26,27]

It should be emphasized that the above models in no way exhaust the range of possible mechanisms of obstructed diffusion that occur in crowded systems, especially in living cells. Different types of anomalous diffusion were observed in the motion of mRNA and gene loci,[28,29] granules in living cells,[30,31] telomeres in nuclei.[32,33] A more extensive review is provided by Höfling and Franosch.[34] In particular, there exist cases when time and ensemble averages show disparate results (ergodicity breaking), an intriguing and still not fully understood feature[35] (see ref 36 for a popular discussion). Also in even better-defined, unbounded systems anomalous diffusion occurs.[37,38] A discussion on the differences between restricted diffusion, which converges to free diffusion at long times, and anomalous diffusion can be found in the simulation study by Soula et al.[39] There is also growing evidence for Brownian yet non-Gaussian diffusion.[40] In a viscoelastic medium such as cytoplasm, anomalous diffusion occurs naturally due to the frequency-dependent degree of anti-persistence (anticorrelation of consecutive increments), although it is not restricted.[41] Therefore, in many systems anomalous diffusion is observed and relevant, and not all sublinear dependence of MSD on time in cells can be attributed to a crossover in restricted Brownian diffusion.

As it has been pointed out by Wawrezinieck et al.,[19] we do not always have enough information about the structure of the crowded medium to be sure which of the above models should be assumed for the analysis of experimental data. In their paper,[19] the authors proposed a method of FCS measurement that was able to distinguish between hop diffusion in square compartments and diffusion in the presence of immobile traps inside which the diffusion coefficient was different than outside. The method boils down to measurement of the dependence of ACF half-time on the varying diameter of the focal volume. However, in many commercially available FCS setups there is no possibility of a continuous variation of that parameter.

Therefore, in this paper we ask whether an FCS experiment with a constant focus size can distinguish between the restricted diffusion described by the above three models. As we will show, all three of them generate nearly the same mean square displacement (MSD). In the theory of FCS, it is often assumed that the autocorrelation function of a restricted diffusion process explicitly depends on the MSD.[7,8,42−45] However, this assumption is only true for diffusive processes that are Gaussian in all time scales: free diffusion (Wiener process) and diffusion in a harmonic potential (Ornstein−Uhlenbeck process).[46,47] When the diffusion is constrained by fully or partially reflecting barriers, the explicit dependence of the ACF on MSD is only an approximation.[47] Are the differences between the ACFs generated by the models (i), (ii), and (iii) large enough to allow the distinction between those models? Which of the parameters of the restricted diffusion process can be accurately retrieved from the FCS measurement if we do not know the underlying model? To answer these questions, we numerically generated trajectories of "particles" moving according to those three models, such that their MSDs are approximately the same. We used these trajectories to perform simulations of FCS experiments and compared their autocorrelation curves. Finally, we tested how well can the diffusion coefficients and confinement sizes be extracted from these curves by fitting the specific models.

THEORY: FCS AUTOCORRELATION FUNCTION

The FCS method is based on the observation of a small volume using a highly focused beam of laser light. Due to electronic excitation, the fluorescent particles in the focal volume emit photons. The intensity of the focused laser light can be approximated by a normal distribution:

$$W(\vec{r}) \approx W_0 \, e^{-2(x^2+y^2)/w_0^2 - 2z^2/z_0^2} \quad (1)$$

where w_0 (radius) and z_0 (semiaxis length) correspond to the distance from the focus center where the light intensity drops down to e^{-2}. In this paper, we assume a three-dimensional

dx.doi.org/10.1021/jp502467u | J. Phys. Chem. B 2014, 118, 4906−4912

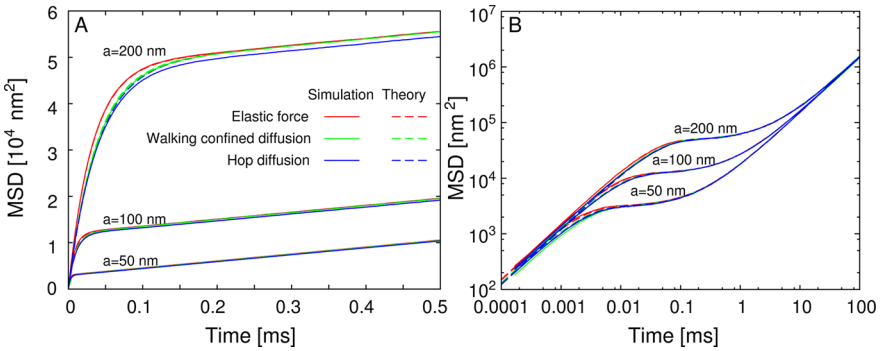

Figure 2. Mean square displacements for diffusion constrained by elastic force, walking confined diffusion, and hop diffusion are nearly the same for the same effective confinement sizes. Because of the difference between spherical and cubic geometry, the effective radius a = 50 in the case of hop diffusion corresponds to the compartment width L = 77.460 nm, a = 100 nm corresponds to L = 154.92 nm, and a = 200 corresponds to L = 309.84 nm. A: Linear scale. B: Log−log scale.

geometry of the observed volume; conversion of our analysis to two dimensions is straightforward. As a result of fluctuations in the concentration of fluorophores, the observed fluorescence intensity varies over time.The autocorrelation of the fluorescence intensities observed in the experiment is

$$G(\tau) = \frac{\int\int W(\vec{r})W(\vec{r}_\tau)\Phi(\vec{r}, \vec{r}_\tau, \tau)d^3r d^3r_\tau}{(C_0\int W(\vec{r})d^3r)^2} \quad (2)$$

where C_0 is an average equilibrium concentration of fluorophores. When the particle motion can be described using a Gaussian propagator,

$$\Phi(\vec{r}, \vec{r}_\tau, \tau) = \frac{1}{\left[\frac{2\pi}{3}\langle\vec{r}^2(\tau)\rangle\right]^{3/2}} e^{-(\vec{r}_\tau-\vec{r})^2/(\frac{2}{3}\langle\vec{r}^2(\tau)\rangle)} \quad (3)$$

where $\langle r^2(\tau)\rangle$ is the mean square displacement, then the autocorrelation function integrates out to the form which explicitly depends on the MSD:

$$G(\tau) = G(\langle r^2(\tau)\rangle) = \frac{1}{N}\left(1 + \frac{2}{3}\frac{\langle r^2(\tau)\rangle}{w_0^2}\right)^{-1}\left(1 + \frac{2}{3}\frac{\langle r^2(\tau)\rangle}{z_0^2 w_0^2}\right)^{-1/2} \quad (4)$$

RESULTS

We numerically generated the MSDs and FCS autocorrelation functions for diffusion constrained by elastic force, walking confined diffusion, and hop diffusion. See Supporting Information (SI) for a detailed description of our simulator algorithm, based on the refs 48−50. We used three different effective radii of the confinement: a = 50, 100, 200 nm, whereas the semiaxes of the focal volume were assumed as typical values for FCS setups: w_0 = 100 nm and z_0 = 500 nm (Table S1 in SI). The diffusion coefficients were: $D_S = 2.5 \times 10^{-10}$ m^2/s and $D_L = 2.5 \times 10^{-12}$ m^2/s. For each confinement size, we averaged the ACFs over five simulations. In the case of the hop diffusion model we averaged over 25 simulations, each with a different, random position of the focal volume.

MSDs of Diffusion Constrained by Elastic Force, Walking Confined Diffusion, and Hop Diffusion Are Approximately the Same. The characteristic feature of all the three cases of restricted diffusion listed in the Introduction is that the motion of the particle would be observed as free diffusion with the coefficient D_S at short time scales, and as free diffusion with a smaller diffusion coefficient D_L at long time scales. In this study, we assume that the time scale of the diffusion inside the confinement and that of the diffusion on a long distance are sufficiently well separated: $D_S \gg D_L$. The MSD for all the three models can be then approximated with a very similar formula (see SI for derivation based on the exact formulas from the refs 51 and 52):

$$\langle r^2(t)\rangle = 6D_L t + \frac{6}{5}a^2(1 - e^{-\gamma(5D_S t)/a^2}) \quad (5)$$

where a is an effective confinement radius. For the elastic force model, a is approximately the mean distance that the particle can travel from the neutral position. For the walking confined diffusion model, a is the radius of the spherical cage. $L/2 = a(3/5)^{1/2} \approx 0.775a$ is the compartment half-width in the hop diffusion model. (Further on, we will use the effective compartment radius a for hop diffusion in some figures for the sake of comparison with the other models.) The exponential decay constant γ slightly differs for the three models: γ = 1 for the model (i), $\gamma \approx 0.866$ for the model (ii), and $\gamma \approx 0.822$ for the model (iii). We numerically generated the trajectories of those three diffusion processes. They have the same long- and short-time diffusion coefficients D_L and D_S, and a very similar shape of MSD (Figure 2). The small difference between the theoretical and simulation curves for hop diffusion at a = 200 nm is due to numerical approximation introduced by the simulation algorithm (see the SI and the discussion later in the text). We note that the asymptotic MSD slope (i.e., the long-time diffusion coefficient D_L) is nevertheless correct.

Large Differences between Positions of the ACF Plateau from Measurement to Measurement Are the Signature of Hop Diffusion. For hop diffusion, a single ACF differs significantly from the averaged ACF, depending on the position of the focal volume with respect to the immobile periodic barriers. In Figure 3 we have shown example ACFs for the confinement width L = 154 nm (a = 100 nm). The focus was centered in two extreme positions, and the middle curve was obtained by averaging over random focus positions. The curves were averaged over 10 realizations and normalized to 1 We can see that the contribution of the long-time diffusion to the curves is small for (0,0,0) and large for (L/2,L/2,L/2). This difference can be explained by the symmetry of the system. Note that the long-time diffusion is a discrete process of transitions between compartments. For the focus position (0,0,0), when a transition occurs through the barrier that lies on the symmetry plane, the correlator does not distinguish transition from reflection. Therefore, only the transitions

dx.doi.org/10.1021/jp502467u | J. Phys. Chem. B 2014, 118, 4906−4912

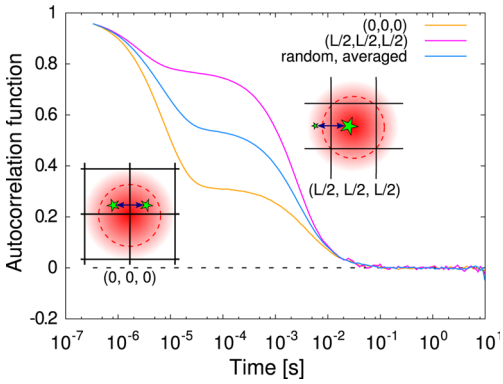

Figure 3. Hop diffusion autocorrelation functions for two extreme positions of the focus and an average over random positions (equal to the average of the two extreme autocorrelation functions). Dotted line denotes the focal volume radius w_0. Both curves are normalized to 1 for comparison.

through the more distant barriers contribute to the long-time diffusion recorded by the correlator, and the apparent confinement size seems to be greater than the actual one.

We therefore conclude that hop diffusion can be suspected when there are large differences between the position of the plateau of ACFs from measurement to measurement. This finding is in agreement with the observations of Wawrezinieck et al.[19]

FCS Autocorrelation Function Depends Mainly on MSD and the Contribution of Higher Moments Is Small. As the first step, we compared the ACFs for the three models (Figure 4). We note that their shapes are similar though not

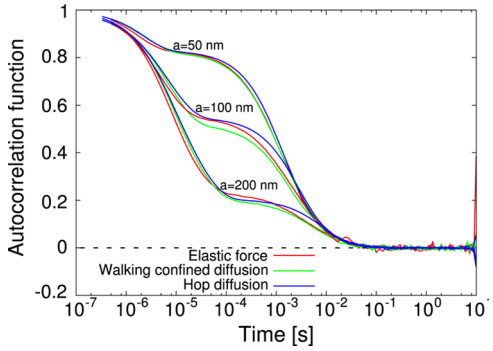

Figure 4. Autocorrelation functions for diffusion confined by elastic force, walking confined diffusion and hop diffusion are similar though not identical. The transient between fast and slow diffusion occurs at a similar time, with differences below 1 order of magnitude.

identical. The transient between fast and slow diffusion occurs at a similar time, with differences below 1 order of magnitude. Under experimental conditions, in the presence of noises, these differences may be difficult to see, especially for the confinement sizes that are much smaller or much larger than w_0 such that the contribution from the restricted diffusion to the overall ACF is very small or very large (see Figure 4). In Figure 4, the curves for the elastic force model have been normalized by fitting the exact formula 4, and then rescaled to 1. The other curves are plotted with the same (rescaled) normalization as that found for the elastic force model for a given confinement size.

Next, we checked whether the simulated ACFs for the specific models can be well approximated by the theoretical ACFs $G(\langle r^2\rangle)$ that depend on the MSD only. In Figure S1 in SI we plotted the simulated ACFs compared with the theoretical ACFs, whose parameters D_L, D_S, and a were same as those used in the simulations: In $G(\langle r^2\rangle_{approx})$ the approximate MSDs (5) are inserted into eq 4, and in $G(\langle r^2\rangle_{simul})$ the MSD generated from simulation is inserted into eq 4. Normalization constants were fitted using the theoretical formulas for corresponding models, with all other parameters fixed at the values used in simulation. Then the normalization was rescaled to 1. For the elastic force model, the ACF indeed depends on the MSD only, and the curve has been shown as a reference to compare it with the curves for the other models. It turns out that the simulated ACFs for walking confined diffusion and hop diffusion differ to some extent from both $G(\langle r^2\rangle_{approx})$ and $G(\langle r^2\rangle_{simul})$, the difference being greater for the hop diffusion model. The differences are not caused by approximation of the MSD given by an infinite series (see eqs 5 and 9 in SI) to a single exponential decay, because $G(\langle r^2\rangle_{approx})$ and $G(\langle r^2\rangle_{simul})$ overlap.

We conclude that, for these non-Gaussian diffusion processes, the dependence of ACF on the second moment of displacement dominates and the contribution of higher moments causes small deviations from the proposed approximate ACF that depends on MSD only.

FCS Does Not Distinguish between Diffusion Constraned by Elastic Force, Walking Confined Diffusion, and Averaged Hop Diffusion. We posed a question whether the small deviations due to higher moments of displacement are sufficient to distinguish between the types of restricted diffusion when the approximate ACF is fitted to the data? To answer this question, we fitted the apparently oversimplified theoretical ACFs for the elastic force model to the simulation data generated by the other models. As the fitting ACF we used $G(\langle r^2\rangle)$ with the MSD given by eq 5 with $\gamma = 1$. The fitting parameters were a, D_S, D_L, and N. The results are shown in Figure 5 and in Table 1. For reference, we also fitted the theoretical ACF for the elastic force model (which, as we know, is accurate) to the simulated data generated by that same model. This allowed us to see whether the deviations of the fitted values from the actual values are random or due to the inaccuracy of the model we used. Judging by the fit quality, the fitted curves overlap with the data almost perfectly. The residues (differences between the fitted and simulated curves) show some systematic deviations, but their magnitude is less than 1.5% of the ACF amplitude. Under experimental conditions, the strong noise present at short times can make them virtually unnoticeable.

We conclude that, despite the small differences between the theoretical and experimental curves, shown in Figure S1 in SI, certain values of a, D_S, and D_L can still be fitted to the data, such that the fit seems to be perfect. We usually do not know *a priori* the exact values of a, D_S, and D_L because they are to be fitted. This means that FCS cannot distinguish between the diffusion constrained by elastic force, walking confined diffusion, and hop diffusion.

Elastic Force Model Correctly Estimates the Parameters of the Other Types of Restricted Diffusion. Can we therefore use the elastic force model as an archetypal model for fitting to the experimental data suspected for restricted diffusion? How much would the fitted parameters a, D_S, D_L

dx.doi.org/10.1021/jp502467u | J. Phys. Chem. B 2014, 118, 4906−4912

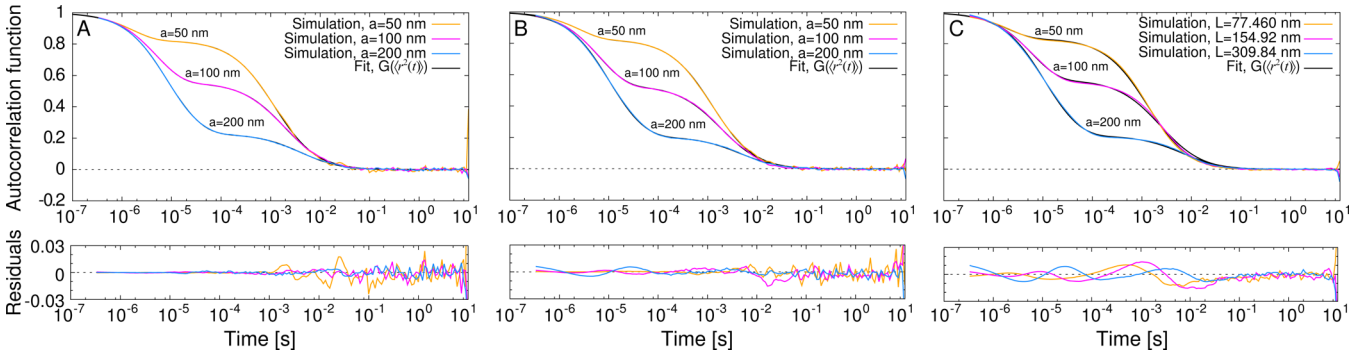

Figure 5. Archetypal model of diffusion constrained by elastic force fitted to the three models of restricted diffusion. (A) Diffusion constrained by elastic force. (B) Walking confined diffusion. (C) Hop diffusion. The fits in B and C seem almost perfect. The residuals (differences between the fitted and simulated curves) show some systematic deviations, but their magnitude is less than 1.5% of the ACF amplitude. The fitting parameters were a, D_S, D_L, N (Table 1). Normalization was later rescaled to 1.

Table 1. Results of Fitting of the Three Models of Restricted Diffusion to the Simulation Data

parameter	actual	fitted, elastic force to elastic force[a]	fitted, elastic force to walking confined diffusion[b]	fitted, elastic force to hop diffusion[c]
a[nm]	50	51.0 ± 0.7	50.6 ± 0.4	49.1 ± 0.6
D_S[10^{-10} m^2/s]	2.5	2.7 ± 0.2	1.75 ± 0.07	2.1 ± 0.1
D_L[10^{-12} m^2/s]	2.5	2.52 ± 0.02	2.45 ± 0.01	2.30 ± 0.02
N	0.1031	0.1039 ± 0.0005	0.1045 ± 0.0003	0.1142 ± 0.0005
a[nm]	100	98.1 ± 0.2	103.0 ± 0.3	95.2 ± 0.4
D_S[10^{-10}m^2/s]	2.5	2.45 ± 0.03	1.96 ± 0.02	1.91 ± 0.04
D_L [10^{-12}m^2/s]	2.5	2.29 ± 0.01	2.49 ± 0.02	1.80 ± 0.02
N	0.1031	0.1036 ± 0.0001	0.1026 ± 0.0002	0.1473 ± 0.0004
a[nm]	200	197.7 ± 0.4	210.4 ± 0.5	205.1 ± 0.6
D_S[10^{-10}m^2/s]	2.5	2.50 ± 0.01	2.05 ± 0.01	1.91 ± 0.01
D_L [10^{-12}m^2/s]	2.5	2.43 ± 0.03	2.43 ± 0.03	1.59 ± 0.03
N	0.1031	0.0986 ± 0.0001	0.1060 ± 0.0001	0.2213 ± 0.0003

[a]The model of diffusion constrained by elastic force fitted to the data generated by the same model. [b]The model of diffusion constrained by elastic force fitted to the data generated by walking confined diffusion. [c]The model of diffusion constrained by elastic force fitted to the data generated by hop diffusion; note that the original size of the compartment is here $L = 2a(3/5)^{1/2}$ = 77.460 nm, 154.92 nm, 309.84 nm.

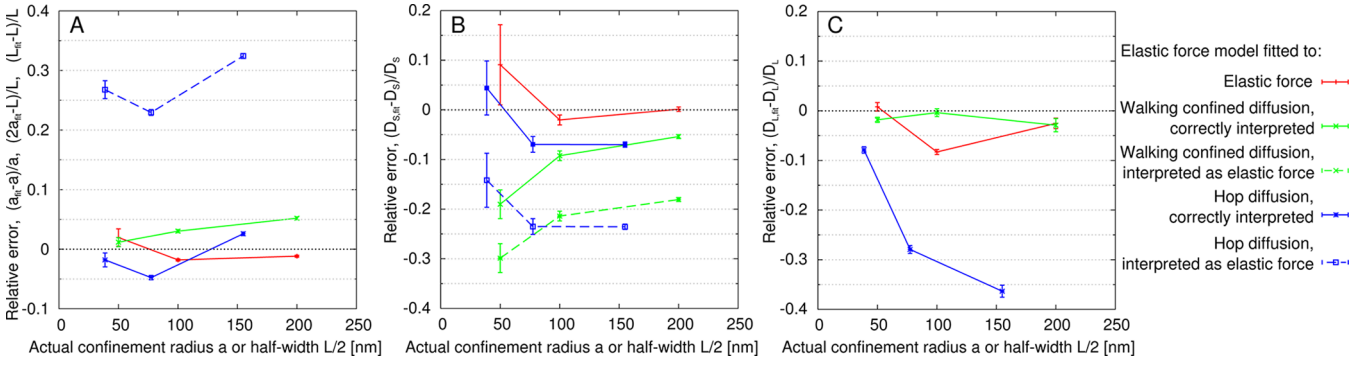

Figure 6. The archetypal model of diffusion constrained by elastic force gives a very good estimation of the confinement size even if it is fitted to the data generated by the other mechanisms of restricted diffusion. The lines connecting data points are used to guide the eye. Solid lines: Relative error of estimation of the confinement size and diffusion coefficients, when the underlying model of diffusion is known. Dashed lines: Relative error of estimation, when the underlying model is unknown and interpreted as the elastic force model. In some cases, the dashed and solid lines overlap. (A) Confinement size. (B) Short-time diffusion coefficient. (C) Long-time diffusion coefficient.

be sensitive to the Gaussian approximation? We analyzed two possibile interpretations of the results:

(a) We have a sufficient knowledge (for example, from microscopy or from single-particle tracking) about the structure of the medium under study to choose *a priori* the underlying model. Then, conversion of the fitting results from the elastic force model to the other models boils down to reinterpretation of the fitted short-time diffusion coefficients $D_{S,model} = D_{S,fit}/\gamma_{model}$. For the hop diffusion model, the confinement width is also converted: $L = 2a(3/5)^{1/2}$.

dx.doi.org/10.1021/jp502467u | J. Phys. Chem. B 2014, 118, 4906−4912

(b) The second possibility is that we do not know which of the three types of restricted diffusion underlies the averaged ACF data. Note that for hop diffusion this may not apply because one can detect this type of diffusion by noticing large differences in the positions of the plateau from measurement to measurement (see Figure 3). In Figure 6 we have shown how well the fitted parameter values reproduce the actual parameters.

In the case (a), the estimation of a (or L) was excellent: For walking confined diffusion the accuracy was less than 5%, and for hop diffusion it was ∼1%. The accuracy for D_S was very good (∼10%) for confinement greater than a half of the focus radius w_0. For smaller confinement sizes, the accuracy of D_S fit was still good (∼20%, note that this uncertainty also affected the reference fit for the exact elastic force model). The estimation of D_L was very good for elastic force and walking confined diffusion models (∼10%), but there was a systematic underestimation of D_L for the hop diffusion model, with the discrepancy growing up to ∼35% with the confinement size.

Can this discrepancy be due to the numerical inaccuracy of the simulation algorithm (see SI)? There are two possible sources of numerical error in our hop diffusion algorithm. The first one is the discrete time step, and we have excluded it using the simulation time step small enough not to influence the shape of the curves. The other one is independent of the time step and it comes from the assumption that the distribution of particle positions inside the confinement is uniform (i.e., the permeability of the barriers is small). As it can be seen in Figure 2, this inaccuracy causes a slightly faster saturation of the diffusive process down to the slow diffusion mode, and it affects the intermediate time scales. The regime of pure long-time diffusion begins only at the end of the autocorrelation curve; moreover it is noisy, so it does not contribute much to the fit. Therefore, looking at the MSD curves, one might suspect that this faster transition to slow diffusion could be the source of underestimation of D_L. However, looking at Figure S1 in SI, dashed lines, we can see that the theoretical curve $G(\langle r^2\rangle_{simul})$, which uses the numerically generated $\langle r^2\rangle_{simul}$ as an argument, decays faster than the simulated ACF, similar to the theoretical curve $G(\langle r^2\rangle_{approx})$. Consequently, the numerical inaccuracy of MSD cannot be the cause of underestimation of D_L. The underestimation of D_L must be therefore connected with the dependence of ACF on higher moments of displacement than the second one (i.e., with non-Gaussianity of the process) and with the averaging over focus positions.

In the case (b), despite the lack of knowledge of the underlying diffusion mechanism, the estimation of a was ∼5% for walking confined diffusion interpreted as diffusion under elastic force. For hop diffusion wrongly interpreted as diffusion constrained as elastic force, the difference was ∼30% due to the geometric factor $(3/5)^{1/2}$ that differentiates the cubic compartment size $L/2$ from the effective size of the spherical domain a, and therefore $(2a - L)/L \approx 29\%$. For D_S the estimation was rather good (between 20% and 30%). The uncertainty of D_L decreased with confinement size from less than 10% down to ∼35%, the same way as in the case (a). Taking into account that the case of hop diffusion could be excluded by checking the differences between single ACFs, as described above, the accuracy of fitting a was excellent. For D_S it was between 20 and 30%, and for D_L it was very good (∼10%).

We also note that for hop diffusion the fitted normalization of the ACFs differs from that predicted for free diffusion, $1/N = l_s^3/(N_s\pi^{3/2}w_0^2z_0)$, where N_s denotes the number of particles in the simulation and l_s denotes the size of the simulation box. The apparent number N of particles in the focal volume increases as the confinement size increases, and it tends to the theoretically predicted value when the confinement size is small (Table 1). This behavior is similar to that found in the ref 11 for impermeable compartments. Theoretically, this might be considered as another signature of hop diffusion, but it can be experimentally useful only if we precisely know the concentration of fluorophores in the studied sample, which is usually not the case.

CONCLUSIONS

This study gives a physical insight into the statistical behavior of the three types of restricted diffusion that are frequently used in the context of biophysics and material science, and into the ability of fluorescence correlation spectroscopy to distinguish between them.

The models of diffusion that we have chosen cover the diversity of possible underlying mechanisms of restricted diffusion. They represent two extremes in terms of statistical behavior: the purely Gaussian process of diffusion under elastic force on the one hand, and the non-Gaussian processes of free diffusion restricted by reflecting boundaries on the other hand. The latter are represented by two qualitatively different models: walking confined diffusion, where the reflecting boundaries themselves diffuse, and hop diffusion, where the boundaries are immobile but permeable, which generates the slow diffusion process in the form of a discrete random walk on a lattice.

We have shown that the three qualitatively different types of restricted diffusion have approximately the same mean square displacement. On the basis of this finding, we have shown by using simulations that the contribution of the second moment of displacement to the averaged FCS autocorrelation function strongly dominates, and the contribution of higher moments is usually too small to allow one to distinguish between the Gaussian or non-Gaussian types of restricted diffusion.

Therefore, the elastic force model can be used as an archetypal model for fitting the fluorescence correlation spectroscopy data suspected of restricted diffusion. The advantage of this model is its simplicity because its autocorrelation function explicitly depends on MSD. Moreover, the MSD in this model contains only one time scale of exponential decay from the fast to slow diffusion. We have shown that, even if the observed diffusive processes are not Gaussian, the Gaussian approximation is sufficient for fitting the confinement size with a very good accuracy, and the estimation of diffusion coefficients is also fairly accurate. This allows one to avoid the use of the exact formulas for ACFs, which are largely unknown (or, if known for special cases, they are based on infinite series, contain special functions and often require numerical integration[10−12,20,53]).

These results help, on the other hand, to better understand the possibilities and limitations of FCS in terms of its ability to capture the statistical properties of diffusive processes. Although FCS can not distinguish between diffusion constrained by elastic force, walking confined diffusion, and hop diffusion averaged over many measurements, one may detect hop diffusion looking at single ACFs by noticing strong differences between the positions of the plateau from measurement to measurement. This effect is caused by different positioning of the focus with respect to the immobile compartments. The presence of immobile compartments also increases the

dx.doi.org/10.1021/jp502467u | J. Phys. Chem. B 2014, 118, 4906−4912

apparent concentration of fluorescent particles, measured by the normalization of ACF.

The limitation of FCS is that it only measures the time correlation of the diffusive motion. Therefore, single particle tracking (SPT) seems to be a very useful complementary technique to obtain additional data when physical interpretation of restricted diffusion is needed. In particular, an inspection of SPT trajectories can give clues about the type of confinement (reflecting or fuzzy) that restricts the motion of particles.

■ ASSOCIATED CONTENT

Supporting Information

Derivation of the mean square displacements. Numerical method of simulation of hop diffusion. Algorithm of the FCS simulator. Supplementary table: Parameters of the simulation. Supplementary figure: Comparison between simulated and theoretical autocorrelation functions. This material is available free of charge via the Internet at http://pubs.acs.org.

■ AUTHOR INFORMATION

Corresponding Author

*E-mail: ochab@ichf.edu.pl.

Notes

The authors declare no competing financial interest.

■ ACKNOWLEDGMENTS

This study was supported by the National Science Centre grant No. 2011/01/D/ST3/00751 (SONATA grant). The authors thank prof. Jacek Gapiński for a helpful discussion.

■ REFERENCES

(1) Rouse, P.; Sittel, K. *J. Appl. Phys.* **1953**, *24*, 690−696.
(2) Knoben, W.; Besseling, N.; Bouteiller, L.; Stuart, M. C. *Phys. Chem. Chem. Phys.* **2005**, *7*, 2390−2398.
(3) Van der Gucht, J.; Besseling, N.; Knoben, W.; Bouteiller, L.; Stuart, M. C. *Phys. Rev. E* **2003**, *67*, 051106.
(4) Raikher, Y. L.; Rusakov, V. V.; Perzynski, R. *Soft Matter* **2013**, *9*, 10857−10865.
(5) Cunha, S.; Woldringh, C. L.; Odijk, T. *J. Struct. Biol.* **2005**, *150*, 226−232.
(6) Daumas, F.; Destainville, N.; Millot, C.; Lopez, A.; Dean, D.; Salome, L. *Biophys. J.* **2003**, *84*, 356−366.
(7) Ochab-Marcinek, A.; Hołyst, R. *Soft Matter* **2011**, *7*, 7366−7374.
(8) Ochab-Marcinek, A.; Wieczorek, S. A.; Ziębacz, N.; Hołyst, R. *Soft Matter* **2012**, *8*, 11173−11179.
(9) Jordan, R.; Lemke, E. A.; Klingauf, J. *Biophys. J.* **2005**, *89*, 2091−2102.
(10) Yeung, C.; Shtrahman, M.; Lun Wuy, X. *Biophys. J.* **2007**, *92*, 2271−2280.
(11) Gennerich, A.; Schild, D. *Biophys. J.* **2000**, *79*, 3294−3306.
(12) Gennerich, A.; Schild, D. *Biophys. J.* **2002**, *83*, 510−522.
(13) Gadd, J. C.; Kuyper, C. L.; Fujimoto, B. S.; Allen, R. W.; Chiu, D. T. *Anal. Chem.* **2008**, *80*, 3450−3457.
(14) Rigler, P.; Meier, W. *J. Am. Chem. Soc.* **2006**, *128*, 367−373.
(15) Kues, T.; Peters, R.; Kubitscheck, U. *Biophys. J.* **2001**, *80*, 2954−2967.
(16) Marguet, M.; Sandre, O.; Lecommandoux, S. *Langmuir* **2012**, *28*, 2035−2043.
(17) Fujiwara, T.; Ritchie, K.; Murakoshi, H.; Jacobson, K.; Kusumi, A. *J. Cell Biol.* **2002**, *157*, 1071−1082.
(18) Heinemann, F.; Vogel, S. K.; Schwille, P. *Biophys. J.* **2013**, *104*, 1465−1475.
(19) Wawrezinieck, L.; Rigneault, H.; Marguet, D.; Lenne, P.-F. *Biophys. J.* **2005**, *1989*, 4029−4042.
(20) Destainville, N. *Soft Matter* **2008**, *4*, 1288−1301.
(21) Dudko, O. K.; Berezhkovskii, A. M.; Weiss, G. H. *J. Phys. Chem. B* **2005**, *109*, 21296−21299.
(22) Raccis, R.; Nikoubashman, A.; Retsch, M.; Jonas, U.; Koynov, K.; Butt, H.-J.; Likos, C. N.; Fytas, G. *ACS Nano* **2011**, *5*, 4607−4616.
(23) Tanaka, S. *Soft Matter* **2012**, *8*, 8936.
(24) Arbe, A.; Colmenero, J.; Alvarez, F.; Monkenbusch, M.; Richter, D.; Farago, B.; Frick, B. *Phys. Rev. Lett.* **2002**, *89*, 245701.
(25) Brás, A. R. E.; Gooß en, S.; Krutyeva, M.; Radulescu, A.; Farago, B.; Allgaier, J.; Pyckhout-Hintzen, W.; Wischnewski, A.; Richter, D. *Soft Matter* **2014**, *10*, 3649−3655.
(26) Jeon, J.-H.; Monne, H. M.-S.; Javanainen, M.; Metzler, R. *Phys. Rev. Lett.* **2012**, *109*, 188103.
(27) Kneller, G. R.; Baczynski, K.; Pasenkiewicz-Gierula, M. *J. Chem. Phys.* **2011**, *135*, 141105.
(28) Golding, I.; Cox, E. C. *Phys. Rev. Lett.* **2006**, *96*, 098102.
(29) Weber, S. C.; Spakowitz, A. J.; Theriot, J. A. *Phys. Rev. Lett.* **2010**, *104*, 238102.
(30) Jeon, J.-H.; Tejedor, V.; Burov, S.; Barkai, E.; Selhuber-Unkel, C.; Berg-Sørensen, K.; Oddershede, L.; Metzler, R. *Phys. Rev. Lett.* **2011**, *106*, 048103.
(31) Tabei, S. M. A.; Burov, S.; Kim, H. Y.; Kuznetsov, A.; Huynh, T.; Jureller, J.; Philipson, L. H.; Dinner, A. R.; Scherer, N. F. *Proc. Natl. Acad. Sci. U.S.A.* **2013**, *110*, 4911−4916.
(32) Bronstein, I.; Israel, Y.; Kepten, E.; Mai, S.; Shav-Tal, Y.; Barkai, E.; Garini, Y. *Phys. Rev. Lett.* **2009**, *103*, 018102.
(33) Burnecki, K.; Kepten, E.; Janczura, J.; Bronshtein, I.; Garini, Y.; Weron, A. *Biophys. J.* **2012**, *103*, 1839−1847.
(34) Höfling, F.; Franosch, T. *Rep. Prog. Phys.* **2013**, *76*, 046602.
(35) Cherstvy, A. G.; Chechkin, A. V.; Metzler, R. *Soft Matter* **2014**, *10*, 1591−1601.
(36) Barkai, E.; Garini, Y.; Metzler, R. *Phys. Today* **2012**, *65*, 29−35.
(37) Szymanski, J.; Weiss, M. *Phys. Rev. Lett.* **2009**, *103*, 038102.
(38) Jeon, J.-H.; Leijnse, N.; Oddershede, L. B.; Metzler, R. *New J. Phys.* **2013**, *15*, 045011.
(39) Soula, H.; Caré, B.; Beslon, G.; Berry, H. *Biophys. J.* **2013**, *105*, 2064−2073.
(40) Wang, B.; Kuo, J.; Bae, S. C.; Granick, S. *Nat. Mater.* **2012**, *11*, 481−485.
(41) Goychuk, I. *Adv. Chem. Phys.* **2012**, *150*, 187.
(42) Schwille, P.; Korlach, J.; Webb, W. *Cytometry* **1999**, *36*, 176−182.
(43) Weiss, M.; Hashimoto, H.; Nilsson, T. *Biophys. J.* **2003**, *84*, 4043−4052.
(44) Weiss, M.; Elsner, M.; Kartberg, F.; Nilssony, T. *Biophys. J.* **2004**, *87*, 3518−3524.
(45) Wu, J.; Berland, K. M. *Biophys. J.* **2008**, *95*, 2049−2052.
(46) Gardiner, C. W. *Stochastic Methods: A Handbook for the Natural and Social Sciences*; Springer: Berlin, 2009.
(47) Enderlein, J. *Phys. Rev. Lett.* **2012**, *108*, 108101.
(48) Pieper, T. Diffusion of fluorescent molecules in micro- and nanostructured environments. Ph.D. thesis, Universität Dortmund: 2007.
(49) Wohland, T.; Rigler, R.; Vogel, H. *Biophys. J.* **2001**, *80*, 2987−2999.
(50) Mannella, R. *Int. J. Mod. Phys. C* **2002**, *13*, 1177−1194.
(51) Horsthemke, W.; Lefever, R. *Noise-Induced Transitions: Theory and Applications in Physics, Chemistry, and Biology*; Springer: Berlin, 2006.
(52) Bickel, T. *Physica A* **2007**, *377*, 24−32.
(53) von der Hocht, I.; Enderlein, J. *Exp. Mol. Pathol.* **2007**, *82*, 142−146.